COO-2458-19

INTERACTIVE GRAPHICS INTERPRETATION OF CALCULATION-MEASUREMENT DISCREPANCIES FOR NEUTRON SPECTRUM MEASUREMENTS IN SODIUM

By

Ansar Parvez and Martin Becker
Department of Nuclear Engineering
Rensselaer Polytechnic Institute
Troy, N. Y. 12181

No. of Pages : 23

No. of Figures : 10

No. of Tables : 1

*Sponsored by USERDA under Contract No. (11-1)-2458

ABSTRACT

Interactive graphic techniques have been employed to analyze and interpret the discrepancies found between the integral measurement and prediction of neutron flux in sodium. Direct adjustments have been made to improve the calculation experiment-agreement in the 10 keV to 1 MeV energy range. In general, the adjusted values for elastic cross sections have been found to be lower than the ENDF/B-IV values. Sensitivity of sodium spectra to the angular distribution of elastically scattered neutrons has also been determined.

I INTRODUCTION

At Rensselaer Polytechnic Institute, integral flux measurements have been carried out in large (effectively infinite) clean assemblies of single materials.[1,2,3] Compared to critical experiments, interpretation of these simple geometry measurements is less complex and the results of these experiments have been usefully employed to assess various neutron data files.[4,5,6] Lately,[7] the effort has been directed to adjust the neutronic data in order to resolve the discrepancies between the calculated and measured neutron spectra more precisely whenever such discrepancies are regarded to be a consequence of inadequacies in differential measurements of neutron cross sections.

Direct data adjustments have been made possible through the development of interactive graphic computing facilities[8] where large volumes of data are displayed and manipulated in an interactive man-machine environment. Further aid is taken from the availability of a simple but viable continuous slowing down theory (CSDT) model[9,10] which complements the more precise transport calculation and facilitates understanding of the complex data-spectrum relationship. Data adjustments are first made on the basis of the CSDT model in the interactive mode and then confirmed by carrying out transport calculations. In Ref. 8, details of the interactive graphic adjustment procedure are given along with the application of these procedures to adjust uranium-238 inelastic cross section and scattering matrices. In this note, we present an analysis of neutron flux measurements in sodium.

II MEASUREMENT AND CALCULATION OF SPECTRA

The details of the experimental setup are described in Ref. 3 and are similar to those for uranium.[2] The neutron source is provided by a beam of electrons generated by the 100 MeV RPI Linear Accelerator and incident upon a target inside a large block of sodium. The neutrons propagate through the medium and are extracted through reentrant holes to be analyzed by the time of flight method. A brief sketch of the experimental assembly and the reentrant holes is shown in Fig. 1. Superimposed on the assembly is the spherical model used in the one dimensional transport calculations employed here to predict the neutron spectra.

The multigroup cross sections and P_8 elastic scattering components for these calculations are generated through SUPERTOG.[11] A weighting spectrum based on the Bn approximation and given by

$$W(u) = \frac{1}{\sigma_t(u) + \frac{2\pi}{N}} \qquad (1)$$

is provided as input to SUPERTOG. The total cross section σ_t used in Eq. 1 is obtained from ENDF/B-IV by using the computer code RESEND[13] and Doppler broadening it through the computer code SIGMA1.[14] One-dimensional discrete ordinate (S_{16}) calculations are carried out through the DTF-IV code.[15] The cuboidal experimental assembly is approximated by a sphere with a diameter of 98 cms (Fig. 1). The experimentally measured source is used in calculations to avoid uncertainties resulting from inadequate prediction of the source. This source spectrum is shown in Fig. 2.

Figure 3 shows the measured spectra in sodium against the 1D, S_{16}, P_8 calculations based on ENDF/B-IV. Neutron spectra at three different positions (marked in Fig. 1) have been chosen to make comparisons. A backward, a transverse, and a close to forward direction, is included. A 49 group structure

extending from 800 eV to 10 MeV (shown in Table 1 as MG11) has been used in the calculations. The following observations can be made from a study of the calculation-measurement comparison shown in Fig. 3.

i) Above 2 MeV there is a gross disagreement between the calculated and measured results. The nature of disagreement varies with the direction of measured flux.

ii) In the energy region below 2 MeV, the overall agreement between the measured and calculated spectra is generally satisfactory on a macroscopic level but discrepancies do exist in predicting the details of the spectrum.

It should be pointed out here that the ENDF/B-IV data for sodium are similar to ENDF/B-III. A calculation-experiment comparison in which the flux calculations were based on ENDF/B-III has already been made by Mallen and Malaviya,[3] and therefore maximum effort in this work will be directed towards the interpretation of the discrepancies found between measurement and calculation of neutron spectra.

III HIGH ENERGY REGION (E>2 MeV)

The large discrepancies at energies higher than 2 MeV have been found to be direction dependent, i.e., they vary in magnitude and sign with the direction. Initial efforts in the understanding of these discrepancies were focused on the angular distribution. Both the elastic and inelastic scattering for sodium show a certain degree of anisotropy. For the purpose of this work the inelastic scattering of neutrons has been assumed to isotropic, while a P_8 approximation has been used to account for the anisotropy of neutrons scattered in elastic collisions. The sensitivity of directional flux to the angular distribution of elastically scattered neutrons has been studied.

In a test case reported here, the ENDF/B-IV angular distribution was modified to obtain a distribution which tended to increase the neutron population in the backward and transverse directions. Figure 4 shows the modified distribution against the ENDF/B-IV distribution. The same figure also shows the shift in the spectrum for the specified change in the angular distribution.

It can be seen that the flux in any direction can be increased by increasing the number of neutron scattered into that direction. However, the change in the flux is limited to the group in which the distribution is modified and does not propagate to the neighboring groups. It does not seem likely that the high energy discrepancies can be accounted for through a reasonable change in the angular distribution.

A likely source of error in the high energy region is the effect of re-entrant holes which are used to facilitate the measurement of spectra in experimental assemblies. Efforts have been made to predict the magnitude of the re-entrant hole perturbations through analytical treatments[16,17] as well as through empirical studies[18] by actually measuring the perturbation in flux following a change in the diameter of the re-entrant hole.

These studies indicate that while the effect is small and negligible at lower energies ($E<4$ MeV), it can be large at higher energies. In view of this fact and the small dependence of spectra on the angular distribution, the high energy discrepancies can be attributed to the presence of re-entrant holes which are not accounted for in the one dimensional discrete solution to the Boltzmann equation. Further investigations along this direction should include application of Monte Carlo techniques to the re-entrant hole problem.

IV INTERMEDIATE AND LOW ENERGY REGION (10 keV<E<2 MeV)

The calculations based on ENDF/B-IV and the 49 group structure MG11 (Table 1) show a disagreement with experiment on a microscopic level. However, this group structure uses very broad groups while sodium shows some narrow and sharp structure in the intermediate and low energy region. To get a better perspective, spectra were recalculated by using the group structure MG22 (again shown in Table 1) which placed most of the groups between 100 keV and 1 MeV. These calculations are compared with the measurements in Fig. 5. Considering the $\mu = 0.84$ direction, one may conclude that the shape agreement is acceptable in the 100 keV - 1 MeV range except around 700 keV and between 250 and 100 keV. The agreement is particularly unsatisfactory below about 200 keV where the measurements show a gradual increase while the calculations increase sharply and then stay more or less constant.

Interactive graphic facilities were used to perform a sensitivity analysis and look for suitable data changes to resolve the discrepancies. The details of this procedure have been given in Ref. 8. In short, the procedure allows one to manipulate any cross section (total or partial) and enables one to study the effect of the data change on the spectrum. The uncertainties assigned to the cross sections are displayed with the cross sections when the adjustments are made

Adjustments in both inelastic and elastic scattering cross sections were considered. The inelastic cross section was found to determine the shape of the spectrum in low MeV range. Although the theory experiment-comparison is not satisfactory in this range, no attempts were made to interpret the discrepancies in terms of inelastic cross section because some of the disagreements in this range may be due to the re-entrant hole effects (Cf. See III).

In the energy region around and below the inelastic threshold (400 keV), the re-entrant hole purturbation is insignificant[18] and these low energy spectra are rather insensitive to the exact angular distribution of elastically scattered neutrons. The discrepancies in this region are not so uniformly distributed as to point towards too high or too low inelastic source. In fact these disagreements revolve around the detailed elastic cross section structure and therefore, it was decided to adjust the elastic scattering cross section. These adjustments in the elastic cross section were strictly limited to resolving the shape and structure discrepancies and caution was excercised to refrain from adjusting the amplitude disagreements since they could have been caused by inadequate prediction of inelastic down scattering sources.

The investigations pointed out that any decrease in the elastic cross section in a particular group increases the flux in that group and at the same time results in a decrease in the flux in the lower groups because fewer neutrons are slowing down out of the group in which the adjustment is made. This secondary effect is more pronounced in sodium than in other materials like uranium or iron. It does not come as a surprise because sodium is a low atomic weight material and neutrons lose more energy in a single elastic collision with sodium than they do in iron or uranium. In certain situations it appeared preferable to manipulate the flux in a particular group by changing the elastic down-scattering from higher groups. This observation provided an important guideline in the data adjustments made to resolve the theory experiment discrepancies shown in Fig. 5.

Figure 6 shows the adjusted elastic cross section (EL111) against the ENDF/B-IV values. The changes in the elastic cross section have been uniformly divided between the secondary distributions resulting from the elastic scattering.

Near the 297 keV minimum, the deviation of the adjusted cross sections from ENDF/B-IV shows qualitative consistency with the differential measurements[19] reported from RPI.

The adjusted cross sections have been checked by performing the DTF-IV calculations. Figure 7 shows the improved agreement between the calculations based on EL111 and the experiment. In the forward and transverse direction the agreement is excellent and an improved shape agreement has resulted in the backward direction.

To extend the shape comparison between experiment and theory to below 100 keV, another set of calculations was carried out by using the group structure MG33 (Cf. Table I). A comparison of measurements and calculations based on this group structure is shown in Fig. 8. Since the 100 keV to 1 MeV region has already been studies, we concentrate here on the region which extends from 10 keV to 100 keV. There is a localized disagreement between experiment and theory. Again, the elastic cross section was adjusted to resolve the discrepancy. This adjusted cross section (E1222) is shown in Fig. 9. This figure is a reproduction of the display generated during the interactive data adjustment. It shows the adjusted elastic cross section against the ENDF/B-IV elastic cross section with error bars representing the assigned uncertainties. These uncertainties have been taken from a Westinghouse report[20] and are primarily based on the differential measurements available at the time ENDF/B version III was evaluated. The purpose of displaying these error bars at this point is to help the analyst realize the magnitude of a 'plausible' data change. Figure 10 is again a reproduction of the display showing the comparison between the measured spectra and the calculated spectra resulting from the use of adjusted elastic cross section (EL222). In the energy region 10 keV to 100 keV where the adjusted data have been employed, theory-experiment discrepancies lie within the uncertainties associated with the integral measurements.

V SUMMARY

Neutron spectrum measurements in sodium have been compared with the discrete ordinate-multigroup calculations based on the ENDF/B-IV data. To include details of the sodium cross section structure, different energy meshes have been employed in the multigroup treatment. Sensitivity of energy spectra to angular distribution of elastically scattered neutrons has been studied. Localized discrepancies found between the measured and calculated spectra (in the 10 keV to 1 MeV range) have been interpreted by making direct-data adjustments to the ENDF/B-IV elastic cross section. While these adjustments are carried out by direct methods in clean and simple experiments, the results are by no means unique. At best, these data adjustments provide quantitative understanding of the discrepances between integral measurements and calculations and establish areas where measurements and/or assessment of differential data should be stressed.

REFERENCES

1. B. K. Malaviya, N. N. Kaushal, M. Becker, E. T. Burns, A. Ginsberg, and E. R. Gaerttner, "Experimental and Analytical Studies of Fast Neutron Transport in Iron," Nucl. Sci. Eng., 47, 329 (1972).

2. N. N. Kaushal, B. K. Malaviya, M. Becker, E. T. Burns, and E. R. Gaerttner, "Measurement and Analysis of Fast Neutron Spectra in Uranium Depleted in in the Uranium-235 Isotope," Nucl. Sci. Eng., 49, 330 (1972).

3. A. N. Mallen, "Measurement and Analysis of Fast and Intermediate Neutron Spectra in a Sodium Assembly," Ph.D. Thesis, Rensselaer Polytechnic Institute, Troy (1973).

4. A. Parvez and M. Becker, "An Assessment of ENDF/B-IV for Iron Based on Integral Measurements," Trans. Am. Nucl. Soc., 24, 454, (1976).

5. M. Becker and N. N. Kaushal, "An Assessment of ENDF/B-III Data for Uranium-238 Based on Integral Spectrum Measurements," Nucl. Sci. Eng., 56, 229 (1975).

6. A. Parvez and M. Becker, "An Assessment of ENDF/B-IV DATA for Uranium," Nucl. Sci. Eng., 62, 571 (1977).

7. A. Parvez and M. Becker, "Direct Data Adjustment for U^{238} by Interactive Graphics Computing," Trans. Am. Nucl. Soc., 22, 717 (1975).

8. A. Parvez and M. Becker, "Use of Interactive Graphic Techniques to Evaluate U^{238} Cross Sections from Integral Measurements," Nucl. Sci. and Eng. (In Press).

9. E. T. Burns and M. Becker, "Fast Neutron Spectrum Models and Their Application to Specific Materials," Trans. Am. Nucl. Soc., 13, 687 (1970).

10. A. Parvez and M. Becker, "Evaluation of Continous Slowing Down Theory Parameters in Highly Absorbing Media," Trans. Am. Nucl. Soc., 25, 111, (1977).

11. R. Q. Wright, J. L. Lucius, N. M. Greene, and C. W. Craven, Jr., "SUPERTOG, A Program to Generate Fine Group Constants and Pn Scattering Matrices from ENDF/B ORNL-TM-2674, Oak Ridge National Laboratory, (1969).

12. M. Becker, "Influence of Deep Minima on Multigroup Cross Section Generation," Nucl. Sci. Eng., 57 , 75 (1975).

13. Odelli Ozer, "Program RESEND," Brookhaven National Laboratory, BNL-17134 January (1972).

14. D. E. Cullen, "Program SIGMA1, (Version 74-1)," Lawrence Livermore Laboratory, UCID-16426, (1974).

15. K. D. Lathrop, "DTF-IV, A Fortran IV Program for Solving the Multigroup Transport Equations with Anisotropic Scattering," LA-3373, Los Alamos Scientific Laboratory (1965).

16. F. McGirt and M. Becker, "The Influence of a Reentrant Hole on Measurements of Fast and Thermal Neutron Spectra," Nucl. Sci. Eng. 39, 56 (1970).

17. M. Danchak, "Re-entrant Hole Effects in Three Dimensional Pulsed Neutron Assemblies," Master Thesis, RPI (1973).

18. N. N. Kaushal and B. K. Malaviya, "Re-entrant Hole Perturbation Effect in Fast Spectrum Measurement in Bulk Media," Linear Accelerator, Project Report, 1969-1970, RPI-328-200, p.p. 149, Rensselaer Polytechnic Institute.

19. P. H. Brown, B. L. Quan, J. J. Weiss, and R. C. Block, "Measurement of Neutron Total Cross-Section of Sodium Near Minima," Trans. Am. Nucl. Soc., 21, 505, (1975).

20. N. C. Paik and T. A. Pitterla,"Evaluation of Sodium-23 Neutron Data for the ENDF/B Version III File," WARD-3045 TAB-2 , (1972).

TABLE I

GROUP TOP ENERGIES (eV)

No.	MG11	MG22	MG33
1	1.0000E 07	1.0000E 07	1.0000E 07
2	7.5000E 06	7.6730E 06	8.8240E 06
3	5.6200E 06	5.8880E 06	7.7880E 06
4	4.2100E 06	4.5180E 06	6.8720E 06
5	3.1600E 06	3.4670E 06	5.3520E 06
6	2.3700E 06	2.6600E 06	4.7230E 06
7	1.7800E 06	2.0410E 06	4.1680E 06
8	1.3300E 06	1.5660E 06	3.6780E 06
9	1.0000E 06	1.2020E 06	3.2460E 06
10	7.5100E 05	1.1350E 06	2.8650E 06
11	5.6300E 05	1.0710E 06	2.2310E 06
12	4.2200E 05	9.5490E 05	1.9690E 06
13	3.1700E 05	9.0150E 05	1.7370E 06
14	2.3700E 05	8.5110E 05	1.5330E 06
15	1.7800E 05	8.0350E 05	1.3530E 06
16	1.3300E 05	7.5850E 05	1.1940E 06
17	1.0000E 05	7.1610E 05	1.0530E 06
18	7.5200E 04	6.7600E 05	8.2080E 06
19	5.6400E 04	6.3820E 05	7.2430E 05
20	4.2300E 04	6.0250E 05	6.3920E 05
21	3.1700E 04	5.6880E 05	5.6410E 05
22	2.3800E 04	5.3700E 05	4.9780E 05
23	1.7800E 04	5.0690E 05	4.3930E 05
24	1.3300E 04	4.7860E 05	3.8770E 05
25	1.0000E 04	4.5180E 05	3.0190E 05
26	7.5300E 03	4.2650E 05	2.6640E 05
27	5.6500E 03	4.0270E 05	2.3510E 05
28	4.2400E 03	3.8010E 05	2.0750E 06
29	3.1800E 03	3.5890E 05	1.8310E 05
30	2.3800E 03	3.3880E 05	1.6160E 05
31	1.7800E 03	3.1980E 05	1.2580E 05
32	1.3400E 03	3.0190E 05	1.1100E 05
33	1.0000E 03	2.8510E 05	9.8030E 04
34	7.5500E 02	2.6910E 05	8.6510E 04
35	5.6600E 02	2.5400E 05	7.6350E 04
36	4.2400E 02	2.3980E 05	6.7370E 04
37	3.1800E 02	2.2640E 05	5.9460E 04
38	2.3800E 02	2.1370E 05	4.6300E 04
39	1.7900E 02	2.0180E 05	4.0860E 04
40	1.3900E 02	1.9050E 05	3.6060E 04
41	1.0000E 02	1.7980E 05	3.1820E 04
42	7.5600E 01	1.6980E 05	2.8080E 04
43	5.6700E 01	1.6030E 05	2.4780E 04
44	4.2500E 01	1.4750E 05	1.9300E 04
45	3.1900E 01	1.3580E 05	1.7030E 04
46	2.3900E 01	1.2500E 05	1.5030E 04
47	1.7900E 01	1.1500E 05	1.3260E 04
48	1.3400E 01	1.0590E 05	1.1700E 04

LIST OF FIGURES

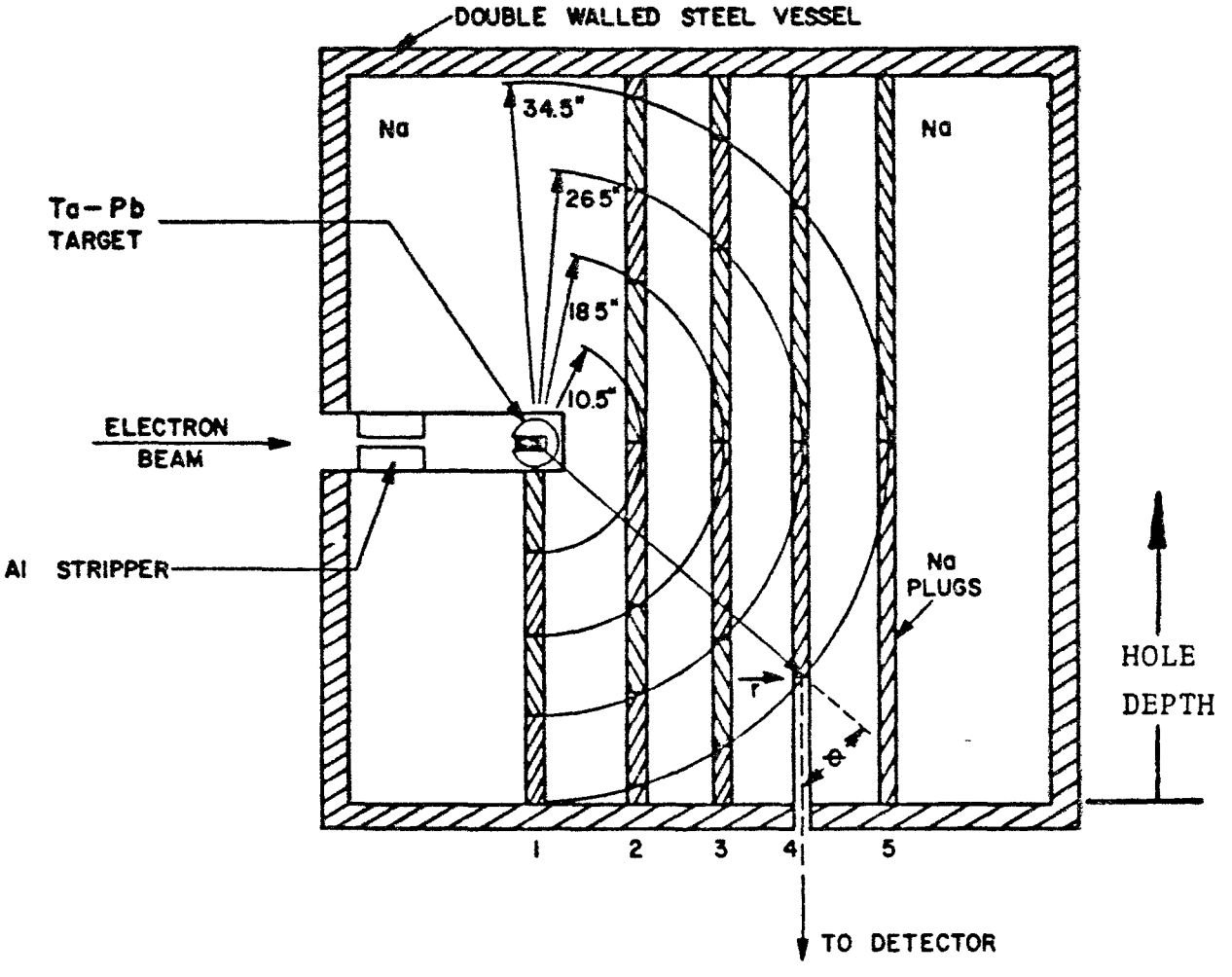
DOUBLE WALLED STEEL VESSEL
Na
34.5"
Na
26.5"
Ta-Pb
TARGET
18.5"
10.5"
ELECTRON
BEAM
Al STRIPPER
Na
PLUGS
HOLE
DEPTH
r
θ
1
2
3
4
5
TO DETECTOR

Figure 1

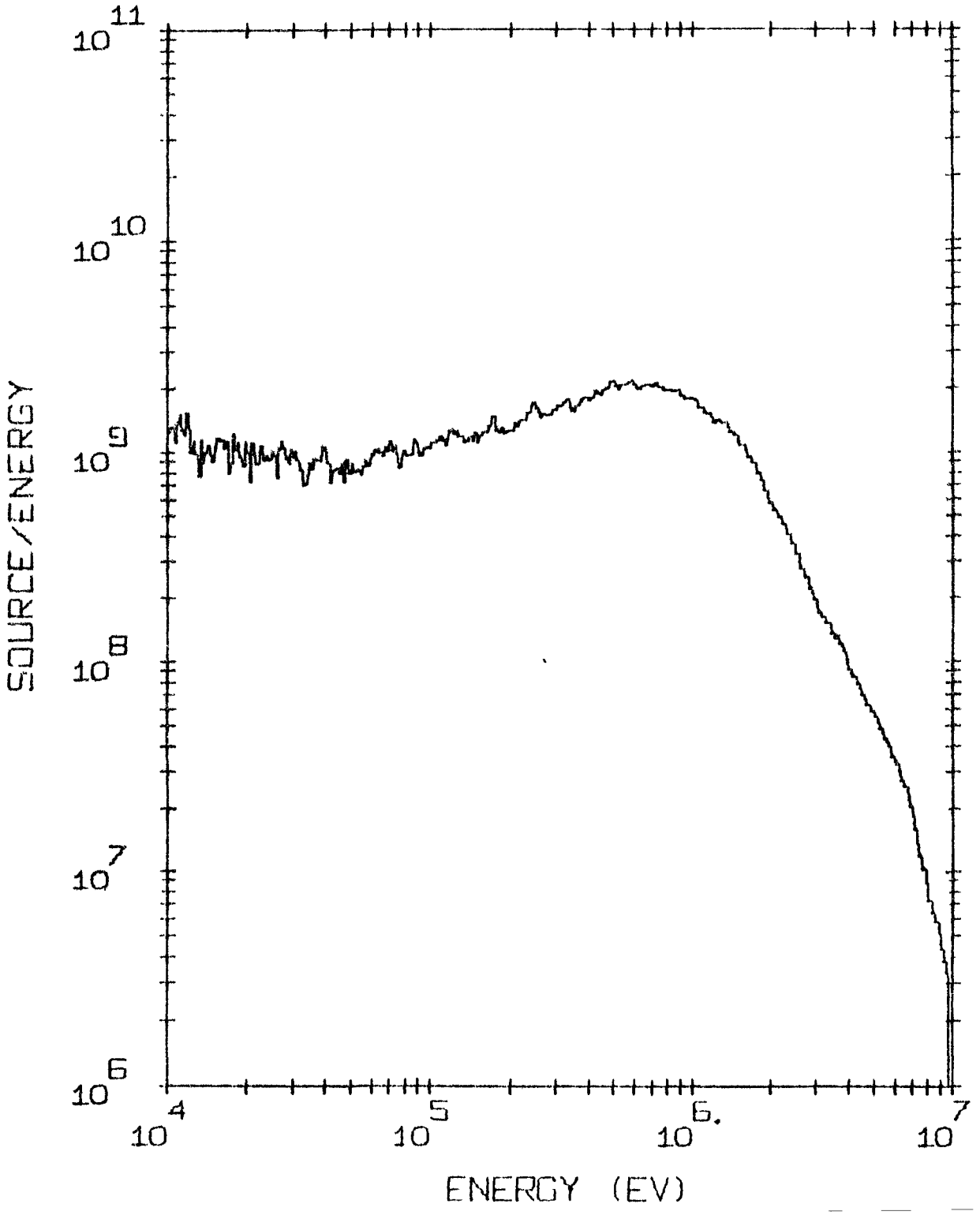
SOURCE/ENERGY
10^11
10^10
10^9
10^8
10^7
10^6
10^4
10^5
10^6
10^7
ENERGY (EV)

Figure 2

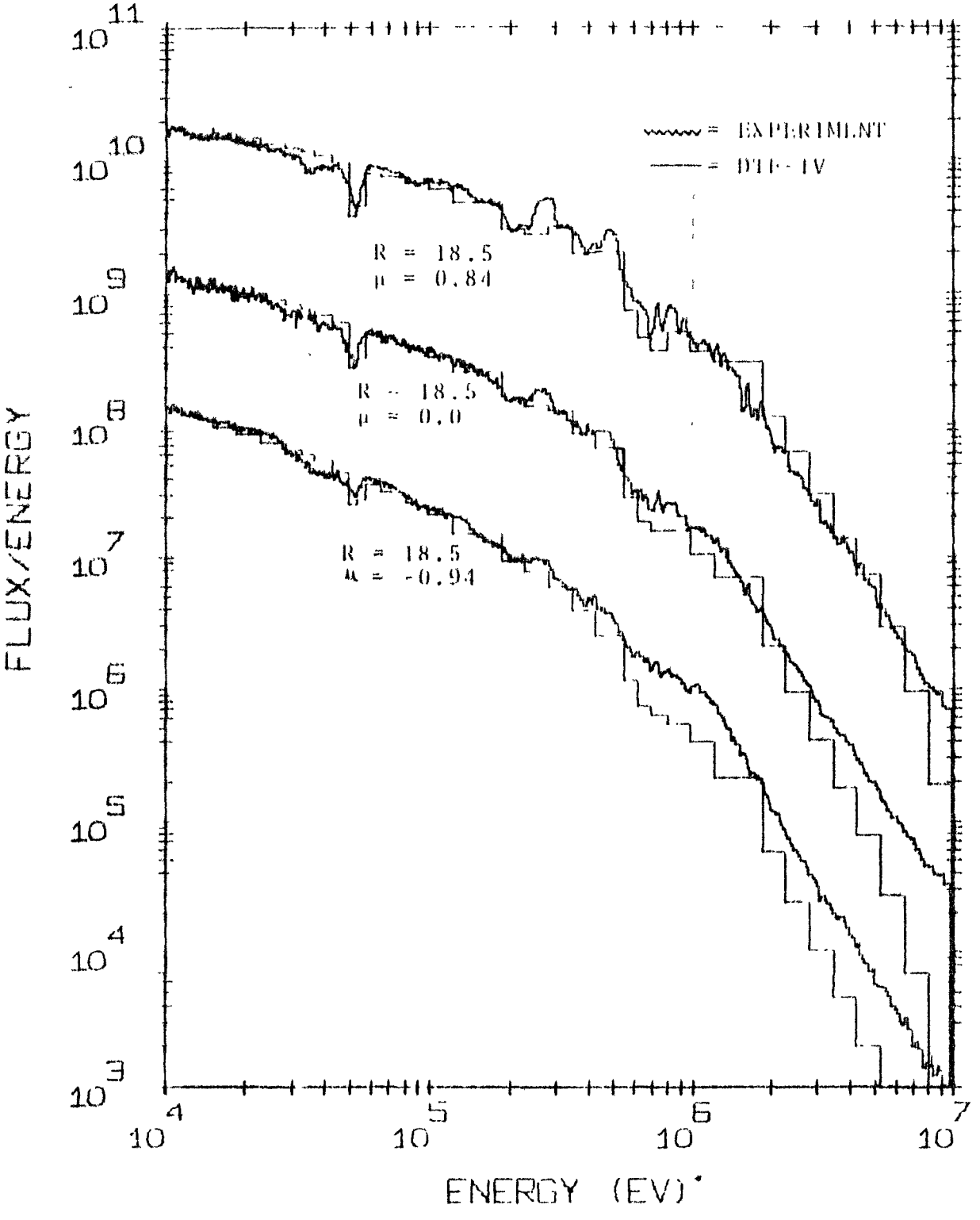
= EXPERIMENT
= DTF-IV
R = 18.5
μ = 0.84
R = 18.5
μ = 0.0
R = 18.5
μ = -0.94
FLUX/ENERGY
ENERGY (EV)
10^11
10^10
10^9
10^8
10^7
10^6
10^5
10^4
10^3
10^4
10^5
10^6
10^7

Figure 3

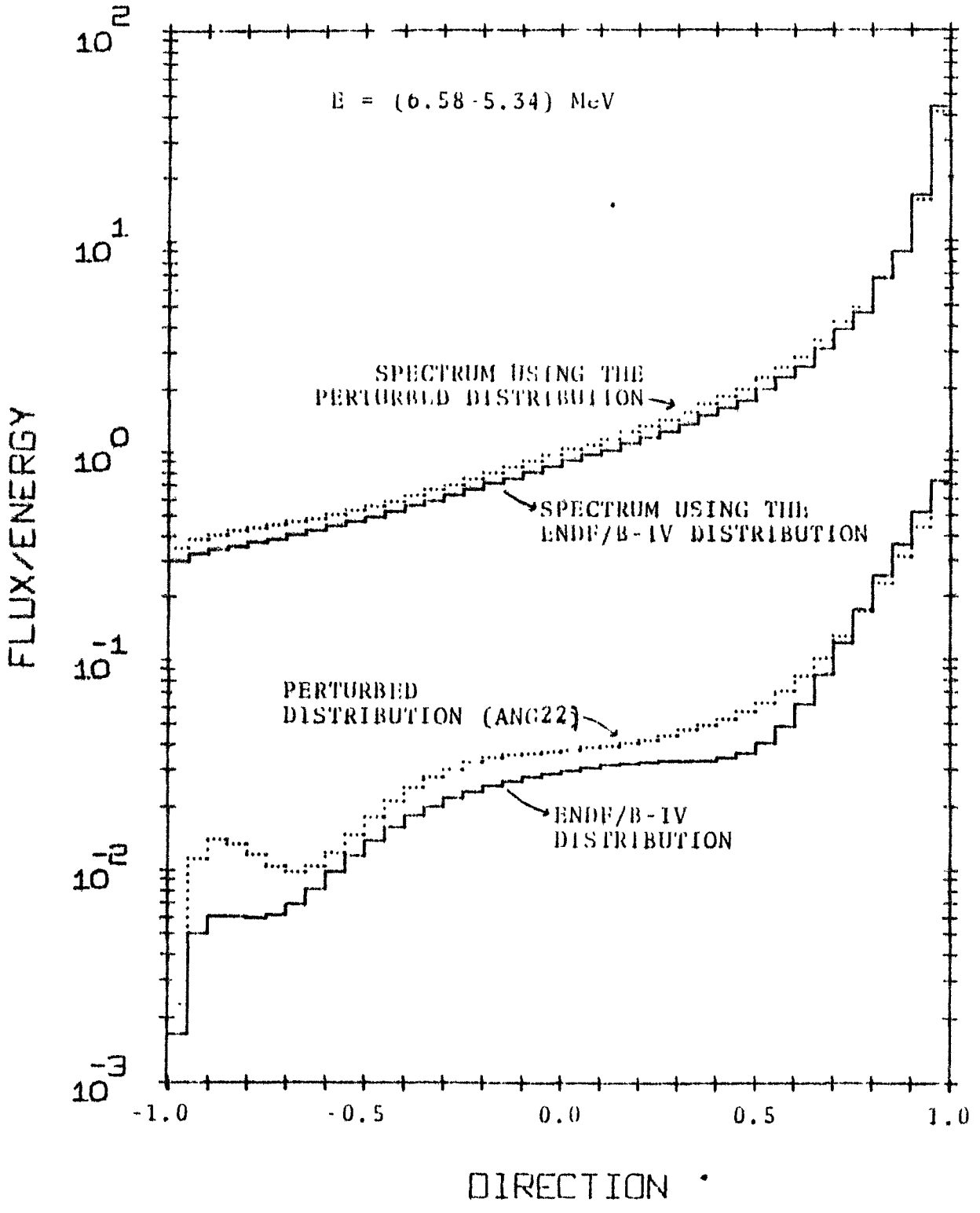
E = (6.58-5.34) MeV
SPECTRUM USING THE PERTURBED DISTRIBUTION
SPECTRUM USING THE ENDF/B-IV DISTRIBUTION
PERTURBED DISTRIBUTION (ANG22)
ENDF/B-IV DISTRIBUTION
FLUX/ENERGY
DIRECTION
10^2
10^1
10^0
10^-1
10^-2
10^-3
-1.0
-0.5
0.0
0.5
1.0

Figure 4

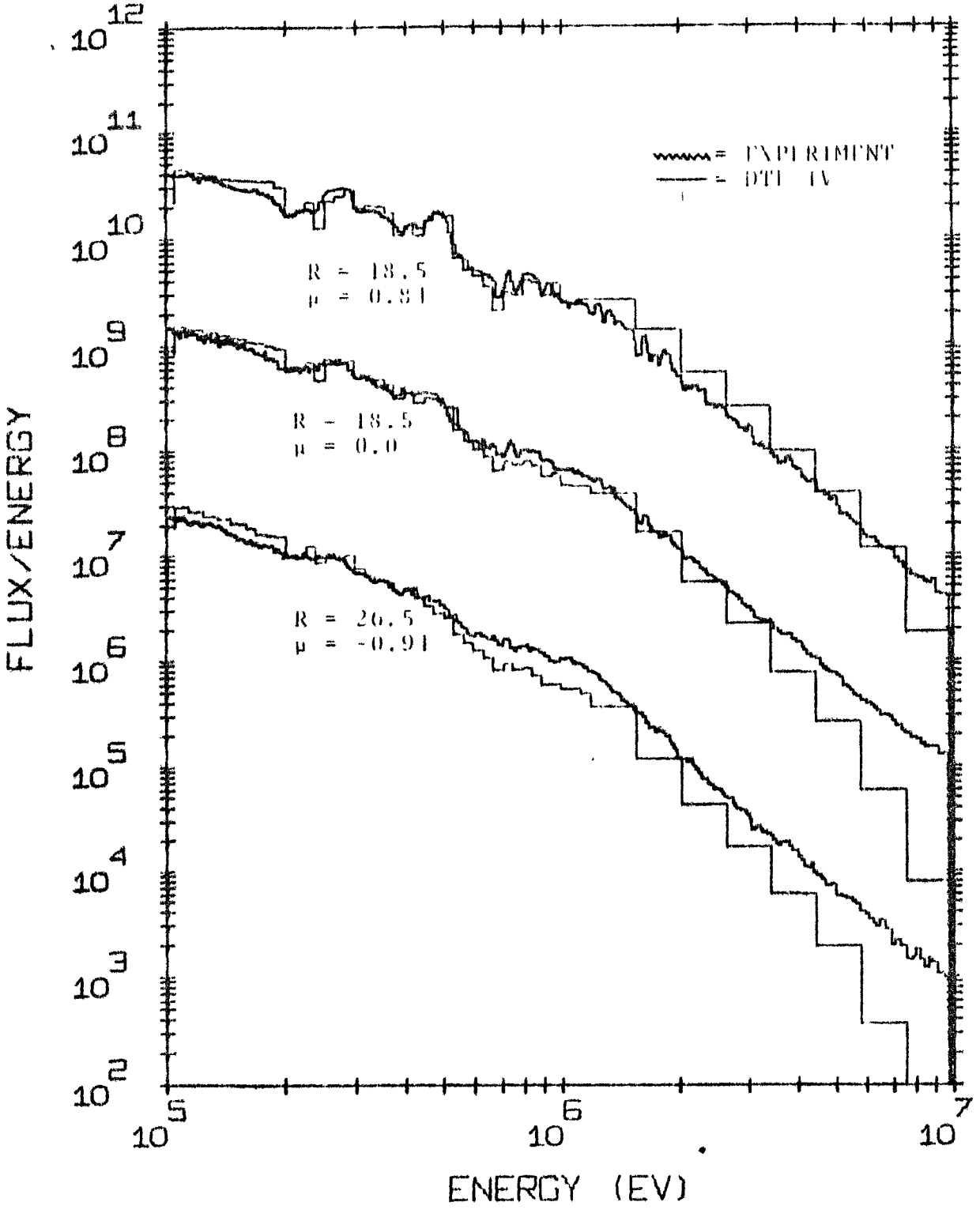
FLUX/ENERGY
ENERGY (EV)
= EXPERIMENT
= DTT IV
R = 18.5
μ = 0.81
R = 18.5
μ = 0.0
R = 26.5
μ = -0.91

Figure 5

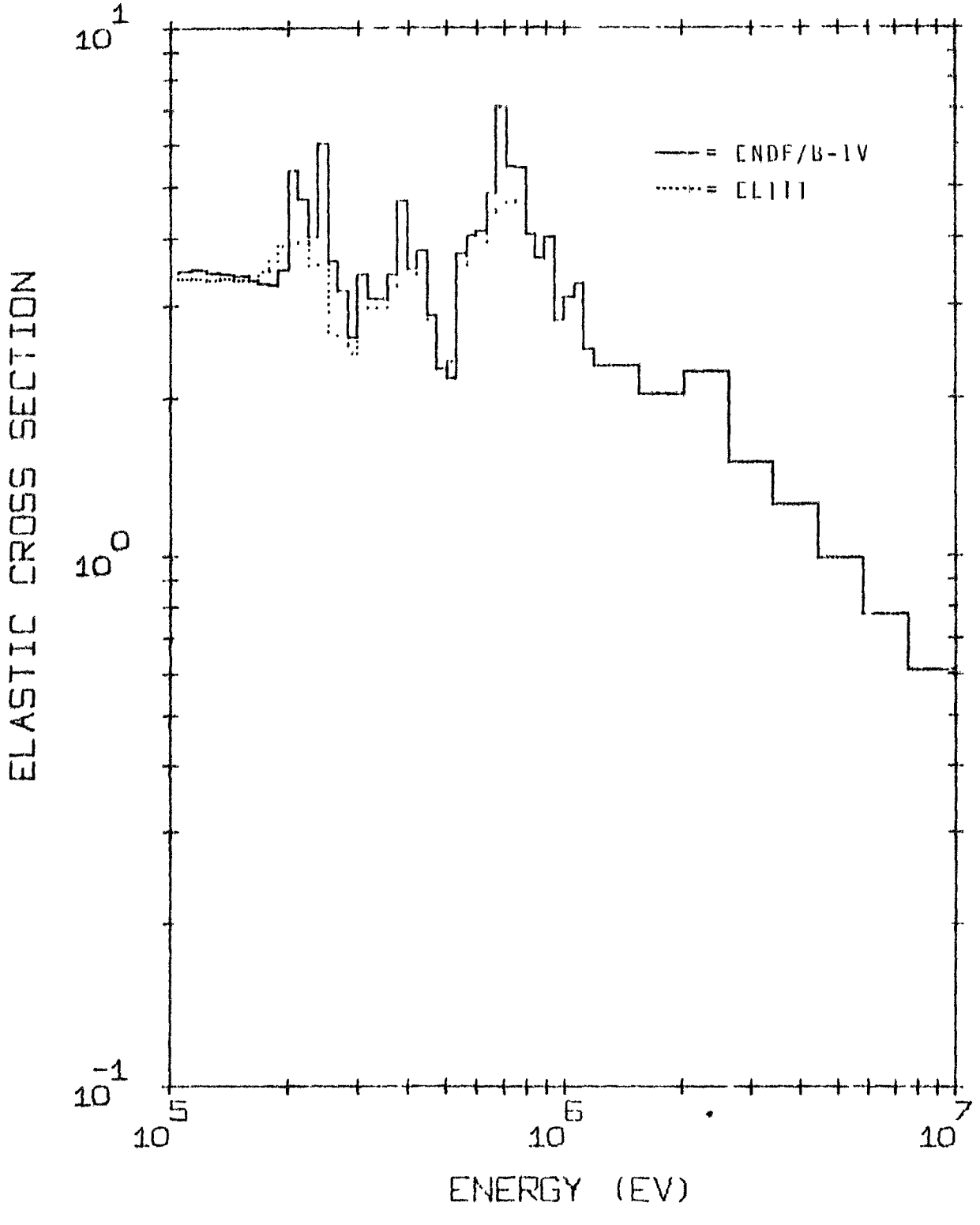
ELASTIC CROSS SECTION
10^1
10^0
10^-1
10^5
10^6
10^7
ENERGY (EV)
= ENDF/B-IV
= ELIII

Figure 6

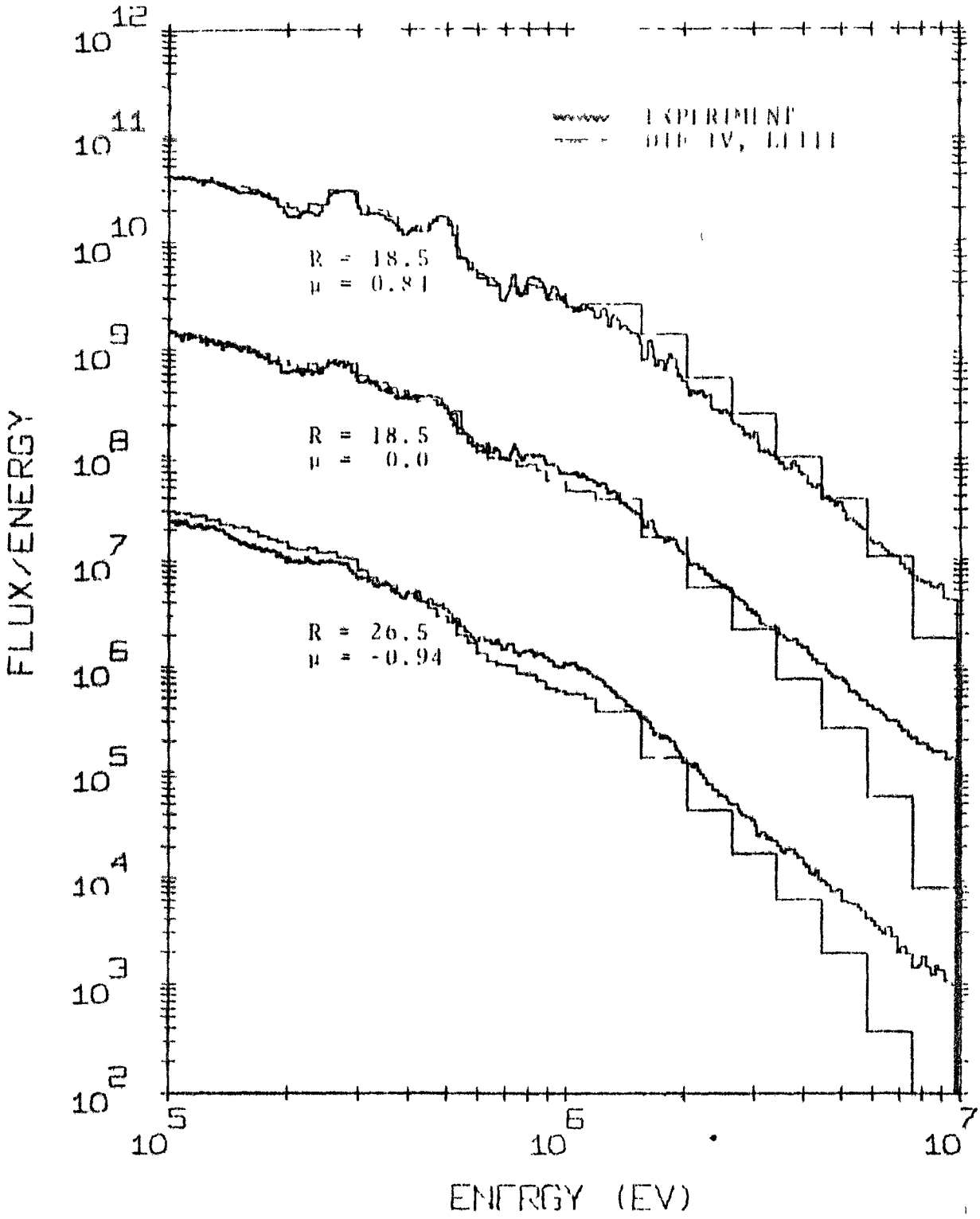
EXPERIMENT
DIF IV, LEVEL
R = 18.5
μ = 0.81
R = 18.5
μ = 0.0
R = 26.5
μ = -0.94
FLUX/ENERGY
ENERGY (EV)
10^12
10^11
10^10
10^9
10^8
10^7
10^6
10^5
10^4
10^3
10^2
10^5
10^6
10^7

Figure 7

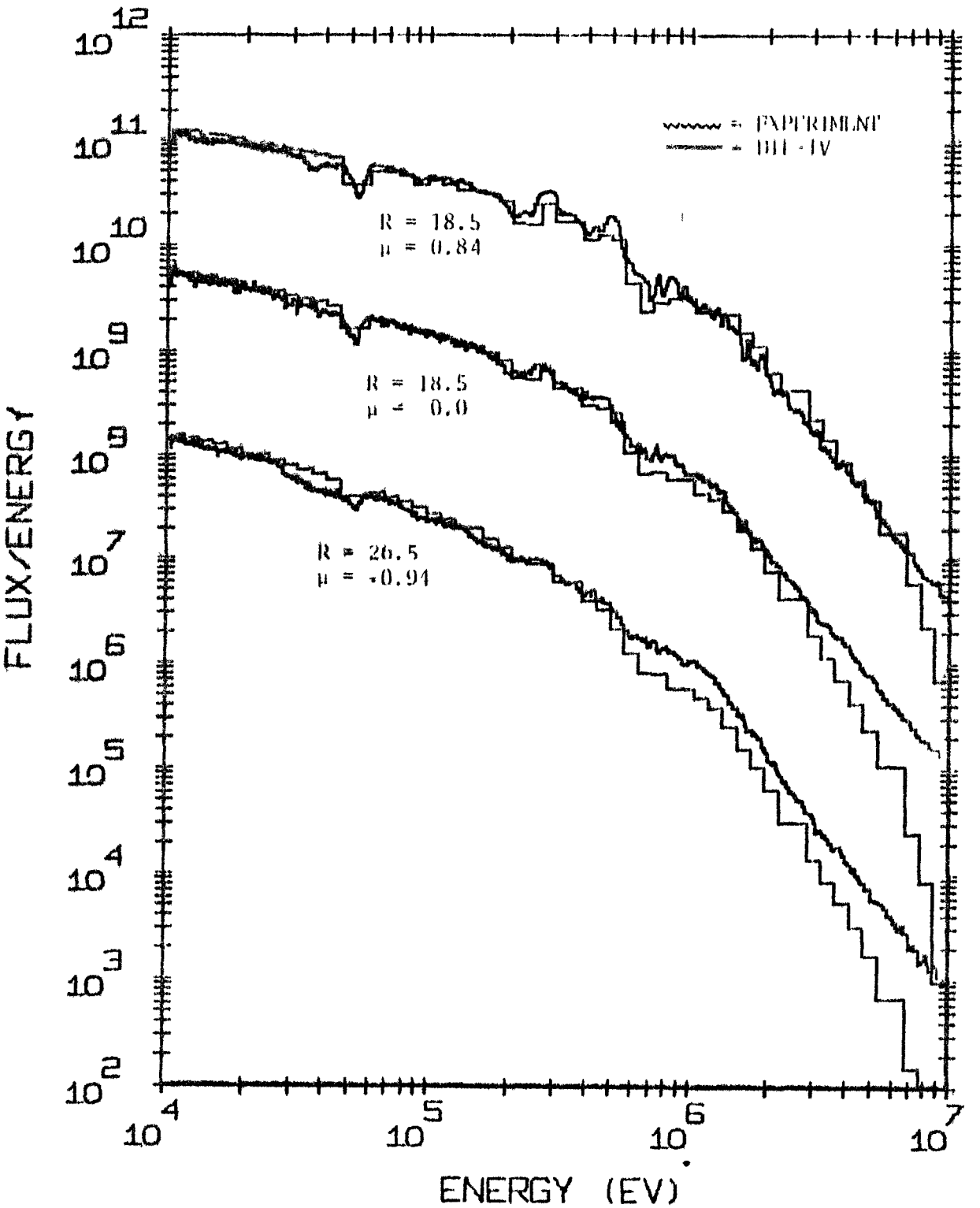

Figure 8

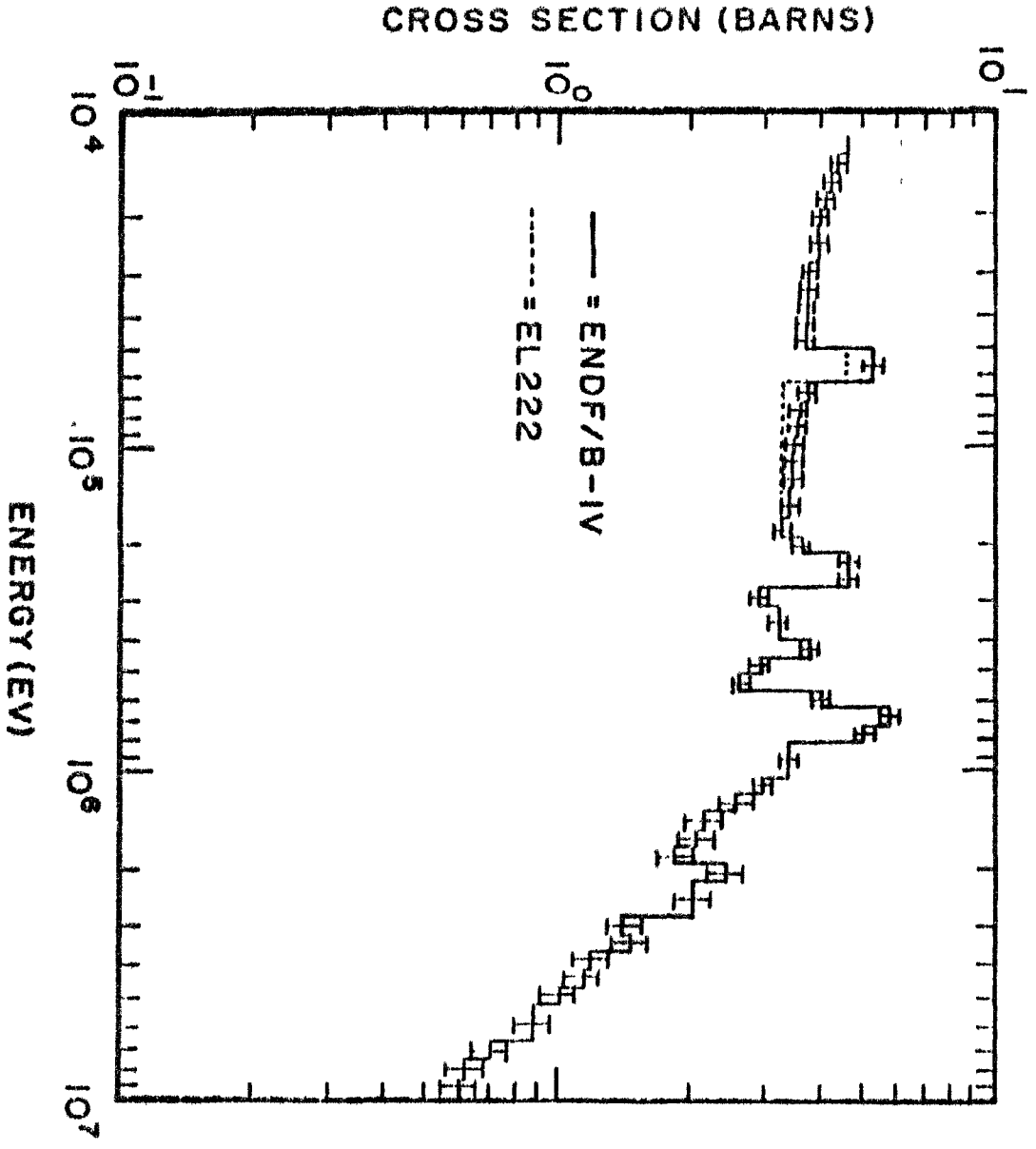
CROSS SECTION (BARNS)
10⁻¹
10⁰
10¹
10⁴
10⁵
10⁶
10⁷
ENERGY (EV)
—— = ENDF/B-IV
----- = EL222

Figure 9

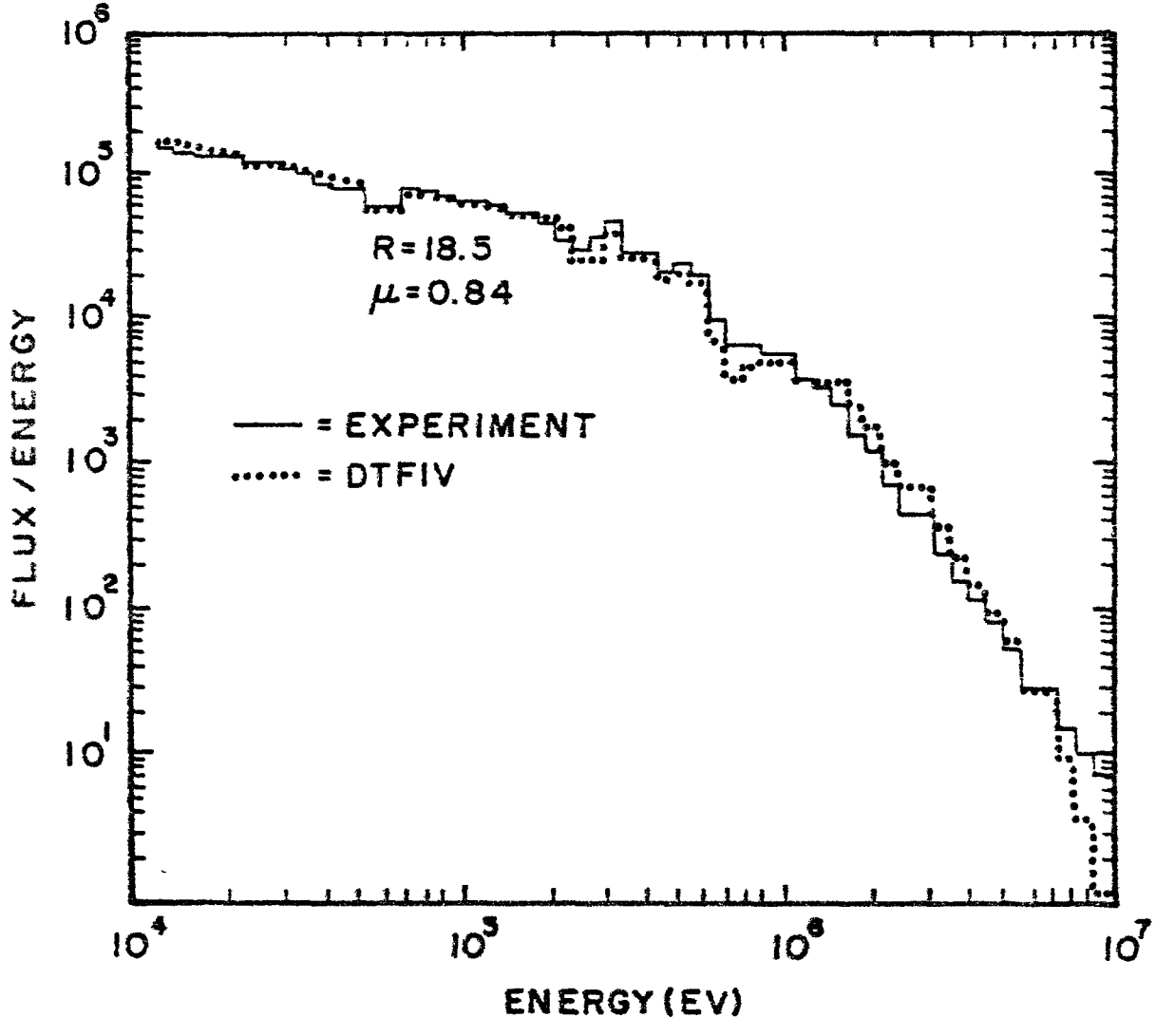

Figure 10